JMEPEG (2014) 23:1580–1584
DOI: 10.1007/s11665-013-0789-3

1059-9495/$19.00

Continuous and Discontinuous αTi Layers Between Grains of β(Ti,Co) Phase

B.B. Straumal, A.S. Gornakova, S.I. Prokofjev, N.S. Afonikova, B. Baretzky, A.N. Nekrasov, and K.I. Kolesnikova

(Submitted October 20, 2013; published online November 26, 2013)

The microstructure of Ti-Co polycrystals with 1.6 and 3.2 at.% Co has been studied between 690 and 810 °C after long anneals (720-860 h) in the αTi+β(Ti,Co) two-phase area of the Ti-Co phase diagram. It has been observed that depending on the annealing temperature and GB energy, the αTi phase forms either chains of separated lens-like precipitates or continuous uniform layers along β(Ti,Co)/β(Ti,Co) GBs. In other words, β(Ti,Co)/β(Ti,Co)GBs completely or partially wetted by the αTi phase were observed. At 690 °C, slightly above eutectoid temperature T_{et} = 685 °C, the portion of the completely wetted β(Ti,Co)/β(Ti,Co) GBs is 25% for the Ti-1.6 at.% Co alloy and 60% for the Ti-3.2 at.% Co alloy. It increases with increasing temperature and reaches the maximum of 80% for the Ti-1.6 at.% Co alloy at 780 °C and of 75% for the Ti-3.2 at.% Co alloy at 750 °C. At 810 °C, i.e., close to the upper border of the αTi + β(Ti,Co) two-phase area of the Ti-Co phase diagram, the portion of the completely wetted β(Ti,Co)/β(Ti,Co) GBs drops down to 40% for the Ti-1.6 at.% Co alloy and 20% for the Ti-3.2 at.% Co alloy. Thus, it has been observed for the first time, that the portion of grain boundaries completely wetted by the layers of a second solid phase can non-monotonously depend on the temperature.

Keywords cobalt, grain boundaries, solid phase, titanium, wetting

1. Introduction

Ti-based alloys have low density, excellent corrosion resistance, and very high tensile strength and toughness even at extreme temperatures. The high strength-to-weight ratio of titanium alloys allows them to replace steel in many applications requiring high strength and fracture toughness. They play an important role as materials for aircrafts, spacecrafts, medical devices, implants, sport cars, etc. Most common are the Ti-V and Ti-Al alloys (Ref 1, 2). Frequently they are additionally doped by other metals (M) like Sn, Nb, Fe, Co, Cr, Cu alone or in various combinations (Ref 1, 2). The parts of Ti-based alloys are commonly produced by the hot working (forging, rolling) in the αTi+ β(Ti,M) two phase area of the Ti-M phase diagrams (Ref 3). The mechanical properties of an alloy during the deformation are critically dependent on the morphology and mutual arrangement of the αTi and β(Ti,M) phases, as well as the degradation processes of these materials during their lifetime.

In turn, the morphology of the interpenetrating polycrystalline phases can be governed by the so-called grain boundary wetting phase transformations. For the liquid droplet on a solid substrate two situations are possible. If a liquid spreads on the surface, one can speak about full (or complete) wetting. The contact angle between liquid and solid in this case is zero. If a liquid droplet does not spread and forms a finite contact angle, it is a partial (or incomplete) wetting. Cahn (Ref 4) and Ebner and Saam (Ref 5) first assumed that the (reversible) transition from incomplete to complete wetting can proceed with increasing temperature, and it is a true surface phase transformation. The recent reviews of the works on the wetting phase transitions can be found in (Ref 6-10).

The transition from incomplete to the complete wetting can also be observed within the grain boundaries (GBs) if the energy of two solid-liquid interfaces 2 σ_{SL} reduces to lower than the GB energy $\sigma_{GB} > 2\ \sigma_{SL}$. Cahn's idea (Ref 4) was the "driving force" for the experimental finding of GB wetting phase transformations, initially made in Zn-Sn, Zn-Sn-Pb, and Ag-Pb polycrystals (Ref 11, 12 and references therein). At a later state, the original experimental data were reconsidered from this point-of-view, and numerous indications on the GB wetting phase transformations were found, particularly for Zn-Sn, Al-Cd, Al-In, Al-Pb (Ref 11 and references therein) and W-Ni, W-Cu, W-Fe, Mo-Ni, Mo-Cu, Mo-Fe (Ref 11, 12 and references therein) polycrystals. The exact measurements of the temperature dependence for the GB contact angle with the melt

This article is an invited submission to JMEP selected from presentations at the Symposia "Wetting," "Interface Design," "Joining Technologies" belonging to the Topic "Joining Interface Design" at the European Congress and Exhibition on Advanced Materials Processes (EUROMAT 2013) held September 8-13 2013 in Sevilla Spain has been expanded from the original presentation.

B.B. Straumal, Institute of Solid State Physics, Russian Academy of Sciences, Ac. Ossipyan str. 2, 142432 Chernogolovka, Russia; Laboratory of Hybrid Nanostructured Materials, National University of Science and Technology «MISIS», Leninskii prosp. 4, 119049 Moscow, Russia; and Karlsruher Institut für Technologie, Institut für Nanotechnologie, Hermann-von-Helmholtz-Platz 1, 76344 Eggenstein-Leopoldshafen, Germany; **A.S. Gornakova, S.I. Prokofjev, N.S. Afonikova,** and **K.I. Kolesnikova**, Institute of Solid State Physics, Russian Academy of Sciences, Ac. Ossipyan str. 2, 142432 Chernogolovka, Russia; **B. Baretzky,** Karlsruher Institut für Technologie, Institut für Nanotechnologie, Hermann-von-Helmholtz-Platz 1, 76344 Eggenstein-Leopoldshafen, Germany; and **A.N. Nekrasov,** Institute of Experimental Mineralogy, Russian Academy of Sciences, Ac. Ossipyan str. 4, 142432 Chernogolovka, Russia. Contact e-mail: straumal@mf.mpg.de.

were made using the individual GBs in the specially grown bicrystals in the Cu-In, Cu-Bi, Al-Sn, Zn-Sn, Al-Zn, Sn-Bi, In-Sn, Zn-Sn, and Zn-In systems (Ref 13-18 and references therein). The GB can also be wetted not by liquid, but by a solid phase like in the Zn-Al (Ref 19), Al-Zn (Ref 13), Al-Mg (Ref 20), Co-Cu (Ref 21), Zr-Nb (Ref 22) alloys and steels (Ref 23) or even by an amorphous phase (Ref 24, 25). The important differences between wetting by a liquid and second solid phases are analyzed in (Ref 9). From the point of view of Cahn's generic phase diagram (Ref 4), the Ti-Co system is quite "suspicious." In other words, it can be expected that the GB wetting by a second solid phase can proceed in the αTi+β(Ti, Co) two phase area of the Ti-Co phase diagram. To investigate this possibility is the goal of our work.

2. Experimental

Ti-Co polycrystals with 1.6 and 3.2 at.% Co has been studied between 690 and 810 °C in the α + β two-phase area of the Ti-Co phase diagram. The alloys was prepared of high purity components (4N Ti and 4N Co) by the levitation melting in vacuum. The 2-mm thick slices were also cut from the ∅ 10 mm cylindrical ingots, then divided into four parts and sealed into evacuated silica ampoules with a residual pressure of approximately 4×10^{-4} Pa at room temperature. Samples were annealed at temperatures 690, 720, 750, 780, and 810 °C for 720-860 h, and then quenched in water. The accuracy of the annealing temperature was ±2 °C. The annealing points were in the two-phase αTi + β(Ti, Co) area of the Ti-Co phase diagram (Fig. 1) (Ref 26). After quenching, samples were embedded in resin and then mechanically ground and polished, using 1-μm diamond paste in the last polishing step, for the metallographic study. After etching, samples were investigated by means of the optical microscopy and by scanning electron microscopy (SEM). SEM investigations have been carried out in a Tescan Vega TS5130 MM microscope equipped with the LINK energy-dispersive spectrometer produced by Oxford Instruments. Light microscopy has been performed using a Neophot-32 light microscope equipped with a 10 Mpix Canon Digital Rebel XT camera. A quantitative analysis of the wetting transition was performed adopting the following criterion: every β(Ti,Co)/β(Ti,Co)GB was considered to be completely wetted only when a layer of αTi-rich film had covered the whole GB (Fig. 2, marked as CW). If such a layer appeared to be interrupted, the GB was regarded as partially wetted (Fig. 2, marked as PW). At least 100 GBs were analyzed at each temperature.

3. Results and Discussion

The spectra of x-rays diffraction are shown in Fig. 3. They reveal that both as-cast and annealed Ti-3.2 at.% Co alloys contain the face-centered cubic (fcc) β-phase and hexagonal α-phase. The as-cast alloy contains about 75% of the hexagonal α-Ti phase with lattice parameters of $a = 2.952$ nm and $c = 4.690$ nm. The remaining 25 % was the fcc β(Ti,Co) phase with lattice parameter of $a = 3.205$ nm. After anneal at 750 °C for 816 h the amount of hexagonal α-Ti phase $a = 2.955$ nm and $c = 4.689$ nm increased to 81 %. The amount of fcc β(Ti,Co) phase $a = 3.201$ nm decreased to 19%.

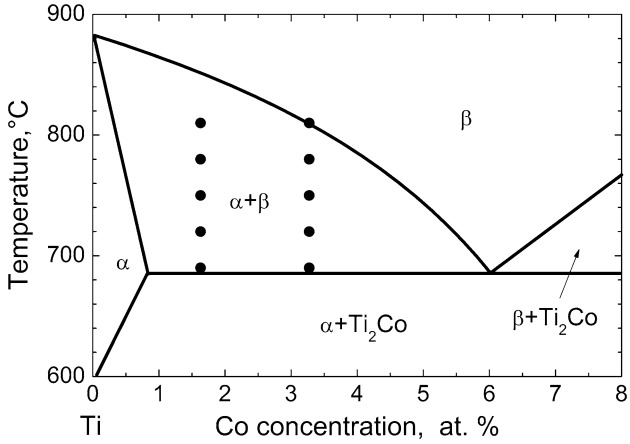

Fig. 1 Part of the Ti-Co phase diagram. Thick lines denote the bulk phase transitions and are taken from (Ref 26). Circles denote the points where the Ti-Co alloys were annealed

SEM micrographs of the Ti-3.2 at.% Co alloy annealed at 750 °C, 816 h and at 780 °C, 864 h are shown in Fig. 2a and b. The β(Ti,Co)grains (matrix) appear light-gray. The αTi phase between β(Ti,Co)grains appear dark-gray. The microstructure of the as-cast alloys (Fig. 3c) contains the fine-grained needle-like mixture of αTi and β(Ti,Co) phases. The needle-like martensitic microstructure appears due the very high cooling rate after levitation melting of the alloys. The β(Ti,Co)/β(Ti,Co)GBs in the as-cast state did not contain neither chains of the αTi particles nor the continuous αTi layers. They formed during the annealing by the bulk and GB diffusion after strong coarsening of primary αTi and β(Ti,Co) lamellae of the starting state. The formation of GB chains or continuous αTi layers proceeds mainly in the first 200-300 h. Afterwards the amount of completely and incompletely wetted GBs did not change much. Therefore, we chosen the annealing duration of 800-900 h in order to measure the equilibrium portion of completely and incompletely wetted β(Ti,Co)/β(Ti,Co) GBs. In Fig. 2a and b, both completely and partially wetted β(Ti,Co)/β(Ti,Co) GBs are visible. The examples of completely (CW) and partially (PW) wetted GBs are shown by arrows. The elongated areas of the αTi phase form chains along the incompletely wetted β(Ti,Co)/β(Ti,Co)GBs (Fig. 2a and b). The majority of β(Ti,Co)/β(Ti,Co)GBs are completely wetted by the αTi phase. In this case, the αTi phase forms the continuous layer separating the β(Ti,Co) grains. A certain remaining amount of αTi phase forms the isolated particles in the bulk of β(Ti,Co) grains.

In Fig. 4, the temperature dependence for the fraction of β(Ti,Co)/β(Ti,Co) GBs completely wetted by the αTi phase is shown. At 690 °C, slightly above eutectoid temperature $T_{et} = 685$ °C, the portion of the completely wetted β(Ti,Co)/β(Ti,Co) GBs is 25% for the Ti-1.6 at.% Co alloy and 60% for the Ti-3.2 at.% Co alloy. It increases with increasing temperature and reaches the maximum of 80% for the Ti-1.6 at.% Co alloy at 780 °C and of 75% for the Ti-3.2 at.% Co alloy at 750 °C. At 810 °C, i.e., close to the upper border of the (αTi + βTi,Co) two-phase area of the Ti-Co phase diagram, the portion of the completely wetted β(Ti,Co)/β(Ti,Co) GBs drops down to 40% for the Ti-1.6 at.% Co alloy and 20% for the

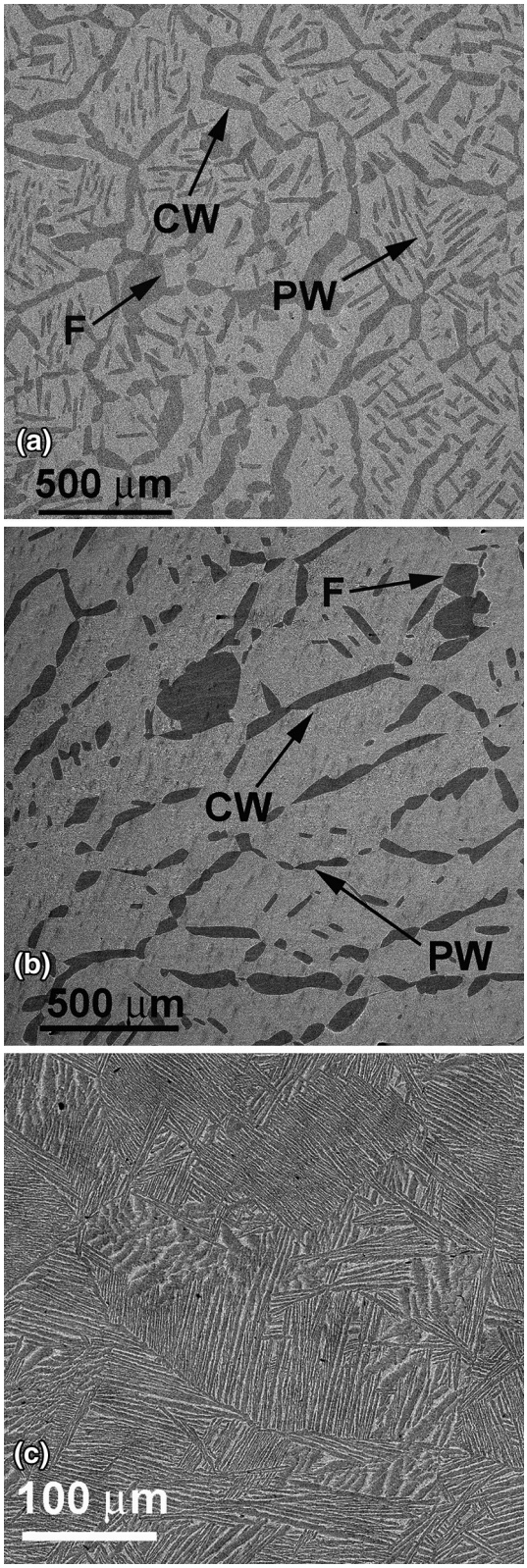

Fig. 2 SEM micrographs of the Ti-3.2 at.% Co alloy. (a) Annealed at 750 °C, 816 h. (b) Annealed at 780 °C, 864 h. (c) As-cast. The β(Ti, Co) grains (matrix) appear light-gray. The αTi phase between β(Ti, Co) grains appears dark-gray. The examples of partially (PW) and completely (CW) wetted β(Ti, Co)/β(Ti, Co) GBs are shown by arrows, as well as faceted αTi/β(Ti,Co) interphase boundaries (F)

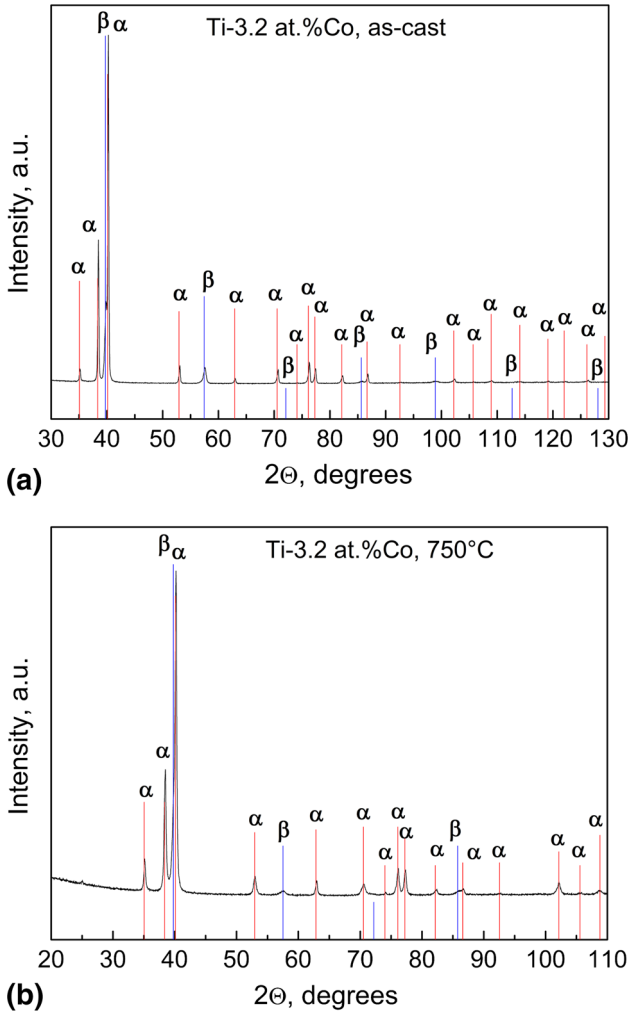

Fig. 3 XRD spectra for the Ti-3.2 at.% Co alloy in the (a) as-cast state and (b) annealed at 750 °C, 816 h

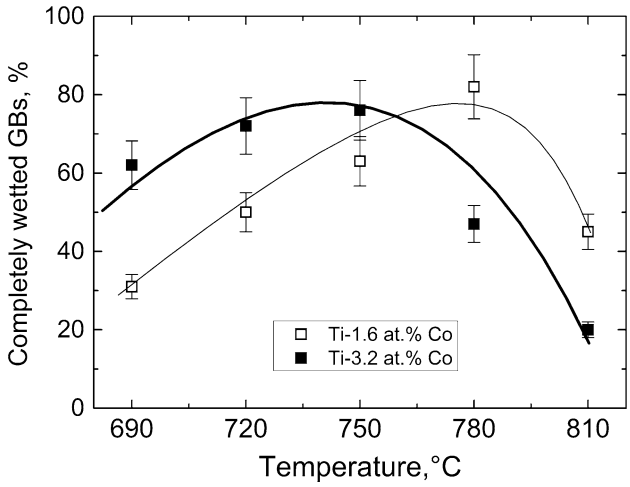

Fig. 4 Portion of β(Ti,Co)/β(Ti,Co) GBs completely wetted by the second solid phase αTi in Ti-1.6 at.% Co (open squares) and Ti-3.2 at.% Co (open squares) at various temperatures. The temperature of eutectoid transformation is T_{et} = 685 °C (Ref 26)

Ti-3.2 at.% Co alloy. The αTi/αTi GBs completely wetted by a layer of β(Ti,Co)phase were not observed in the studied samples.

At each temperature above T_{et} both completely and partially wetted GBs exist. Most probably this difference is due to the scatter of specific enthalpy (excess energy for the unit area) of different β(Ti,Co)/β(Ti,Co)GBs. For example, we observed earlier that the GBs with low energy (like twin GBs) cannot be completely wetted by a second solid phase and contain only the chains of the solid particles instead of continuous layers of a second solid phase (Ref 19). The relative quantity of a second phase can in principle influence the amount of completely wetted GBs (Ref 27). However, the experimental points in Fig. 4 for two different alloys do not scatter much. It means that in the studied concentration and temperature interval the influence of the relative quantity of a second phase is low.

Why the portion of β(Ti,Co)/β(Ti,Co) GBs completely wetted by a second solid phase α(Ti) non-monotonously depends on the temperature (Fig. 4)? If the second, wetting phase is liquid, the energy of two solid-liquid interfaces $2\sigma_{SL}$ always decreases with increasing temperature steeper than the GB energy σ_{GB}. It is just because the entropy of a melt is always higher than that of a solid phase, independently on the misorientation and inclination of grain and interphase boundaries. If the second, wetting phase is solid, the entropy restriction is not valid, and σ_{GB} can decrease with increasing temperature quicker than 2 $\sigma_{\alpha\beta}$, being the energy of interphase boundary between α and β solid phases. In this case the transition from partial to complete GB wetting would proceed not by the temperature increase, but by decreasing temperature, like it happens in the Al-Zn alloys (Ref 13). The additional second-order phase transformations in the bulk do not change the lattice structure of both solid phases but can influence the $\sigma_{GB}(T)$ and $2\sigma_{\alpha\beta}(T)$ dependences. As a result, the $\sigma_{GB}(T)$ and 2 $\sigma_{\beta}(T)$ curves can intersect twice, like in case of transition from paramagnetic Co to ferromagnetic Co in the Co-Cu system (Ref 21).

In case of Co-Cu alloys, the additional ferromagnetic attraction between adjacent cobalt grains "squeezes" the non-ferromagnetic copper layer and prevents the complete wetting of Co/Co GBs by copper. It is similar to the disappearance of the Zn-rich premelting GB layer below the Curie temperature in the specially grown Fe-Si bicrystals (Ref 28-30). This phenomenon led to the non-monotonous dependence of the portion of Co/Co GBs completely wetted by Cu layers around Curie-temperature in Co (Ref 21).

In our case, the second-order phase transformations similar to those in Fe-Si alloys (Ref 29, 30) proceed neither in αTi nor in β(Ti,Co). Nevertheless, the temperature dependence of the portion of β(Ti,Co)/β(Ti,Co) GBs completely wetted by αTi layers is non-monotonous. Indeed, the dependence in Fig. 4 results from a superposition of transitions from partial to complete GB wetting for individual GBs. It is well known that both σ_{GB} and $2\sigma_{SL}$ drastically depend on the GB misorientation angles (Ref 31-36). The good visible faceting of β(Ti,Co)/β(Ti,Co) GBs and αTi/β(Ti,Co) interphase boundaries (Fig. 2) forces us to recollect that σ_{GB} and $2\sigma_{SL}$ are also inclination-dependent, especially in the metals with hexagonal lattice like αTi (Ref 37-39). The scatter of σ_{GB} and $2\sigma_{SL}$ leads not only to the scatter in T_w values (Ref 14-16). It is also possible that for certain GBs the transition from partial to complete wetting proceeds by the increasing temperature, and for another GBs it proceeds by decreasing temperature. The superposition of these two types of thermal dependences would finish in the non-monotonous behavior of temperature dependence for the portion of completely wetted GBs. If it is the case, it is quite possible that such non-monotonous change of the portion of completely wetted GBs will be observed also in other Ti-based alloys. However, at the moment the reasons of non-monotonous temperature dependence of the portion of completely wetted GBs are not known exactly. This unusual non-monotonous temperature dependence deserves the detailed investigation in the future.

4. Conclusions

1. The morphology of the αTi layers (precipitates) in the β(Ti,Co)/β(Ti,Co)GBs has been thoroughly investigated for the first time.
2. It has been observed that the αTi phase can either completely or partially wet the β(Ti,Co)/β(Ti,Co)GBs in the αTi + β(Ti,Co) two-phase field of the Ti-Co phase diagram.
3. It has been observed for the first time that the portion of β(Ti,Co)/β(Ti,Co) grain boundaries completely wetted by the layers of a second solid phase αTi can non-monotonously depend on the temperature.
4. At 690 °C, slightly above eutectoid temperature T_{et} = 685 °C, the portion of the completely wetted β(Ti,Co)/β(Ti,Co) GBs is 25% for the Ti-1.6 at.% Co alloy and 60% for the Ti-3.2 at.% Co alloy. It increases with increasing temperature and reaches the maximum of 80% for the Ti-1.6 at.% Co alloy at 780 °C and of 75% for the Ti-3.2 at.% Co alloy at 750 °C. At 810 °C, i.e., close to the upper border of the (αTi + βTi,Co) two-phase area of the Ti-Co phase diagram, the portion of the completely wetted β(Ti,Co)/β(Ti,Co) GBs drops down to 40% for the Ti-1.6 at.% Co alloy and 20% for the Ti-3.2 at.% Co alloy.
5. We supposed that the non-monotonous thermal behavior of the portion of GBs completely wetted by a second solid phase can be controlled by the superposition of ascending and descending temperature dependences of a contact angle for GBs with different character (misorientation, inclination).

Acknowledgments

The work was partially supported by the Russian Foundation for Basic Research (Grants 12-03-00894 and 13-08-90422) and by the Russian Federal Ministry for Education and Science (Grant 14.A12.31.0001).

References

1. R. Boyer, E.W. Collings, and G. Welsch, *Materials Properties Handbook: Titanium Alloys*, ASM International, Materials Park, 1994
2. M. Geetha, A.K. Singh, R. Asokamani, and A.K. Gogia, Ti Based Biomaterials, the Ultimate Choice for Orthopaedic Implants, *Prog. Mater. Sci.*, 2009, **54**, p 397–425
3. M.J. Donachie, Jr., *Titanium: A Technical Guide*, 2nd ed., ASM International, Materials Park, 2000
4. J.W. Cahn, Critical Point Wetting, *J. Chem. Phys.*, 1977, **66**, p 3667–3676

5. C. Ebner and W.F. Saam, New Phase-Transition Phenomena in Thin Argon Films, *Phys. Rev. Lett.*, 1977, **38**, p 1486–1489
6. D. Bonn, J. Eggers, J. Indekeu, J. Meunier, and E. Rolley, Wetting and Spreading, *Rev. Mod. Phys.*, 2009, **81**, p 739–805
7. M. Tang, W.C. Carter, and R.M. Cannon, Diffuse Interface Model for Structural Transitions of Grain Boundaries, *Phys. Rev. B*, 2006, **73**, p 024102
8. J. Luo, M. Tang, R.M. Cannon, W.C. Carter, and Y.M. Chiang, Pressure-Balance and Diffuse-Interface Models for Surficial Amorphous Films, *Mater. Sci. Eng. A*, 2006, **422**, p 19–28
9. W.D. Kaplan, D. Chatain, P. Wynblatt, and W.C. Carter, A Review of Wetting Versus Adsorption, Complexions, and Related Phenomena: The Rosetta Stone of Wetting, *J. Mater. Sci.*, 2013, **48**, p 5681–5717
10. J. Luo, Stabilization of Nanoscale Quasi-Liquid Interfacial Films in Inorganic Materials: A Review and Critical Assessment, *Crit. Rev. Solid State Mater. Sci.*, 2007, **32**, p 67–109
11. N. Eustathopoulos, Energetics of Solid/Liquid Interfaces of Metals and Alloys, *Int. Met. Rev.*, 1983, **28**, p 189–210
12. B.B. Straumal, *Grain Boundary Phase Transitions*, Nauka publishers, Moscow, 2003 (In Russian)
13. S.G. Protasova, O.A. Kogtenkova, B.B. Straumal, P. Zięba, and B. Baretzky, Inversed Solid-Phase Grain Boundary Wetting in the Al-Zn System, *J. Mater. Sci.*, 2011, **46**, p 4349–4353
14. B. Straumal, T. Muschik, W. Gust, and B. Predel, The Wetting Transition in High and Low Energy Grain Boundaries in the Cu(In) System, *Acta Metall. Mater.*, 1992, **40**, p 939–945
15. B. Straumal, D. Molodov, and W. Gust, Wetting Transition on the Grain Boundaries in Al Contacting with Sn-rich Melt, *Interface Sci.*, 1995, **3**, p 127–132
16. B. Straumal, W. Gust, and T. Watanabe, Tie Lines of the Grain Boundary Wetting Phase Transition in the Zn-rich Part of the Zn-Sn Phase Diagram, *Mater. Sci. Forum*, 1999, **294–296**, p 411–414
17. B.B. Straumal, A.S. Gornakova, O.A. Kogtenkova, S.G. Protasova, V.G. Sursaeva, and B. Baretzky, Continuous and Discontinuous Grain Boundary Wetting in the Zn-Al System, *Phys. Rev. B*, 2008, **78**, p 054202
18. L.S. Chang, E. Rabkin, B.B. Straumal, S. Hoffmann, B. Baretzky, and W. Gust, Grain Boundary Segregation in the Cu-Bi System, *Defect Diff. Forum*, 1998, **156**, p 135–146
19. G.A. López, E.J. Mittemeijer, and B.B. Straumal, Grain Boundary Wetting by a Solid Phase: Microstructural Development in a Zn-5 wt.% Al Alloy, *Acta Mater.*, 2004, **52**, p 4537–4545
20. B.B. Straumal, B. Baretzky, O.A. Kogtenkova, A.B. Straumal, and A.S. Sidorenko, Wetting of Grain Boundaries in Al by the Solid Al_3Mg_2 Phase, *J. Mater. Sci.*, 2010, **45**, p 2057–2061
21. B.B. Straumal, O.A. Kogtenkova, A.B. Straumal, Y.O. Kuchyeyev, and B. Baretzky, Contact Angles by the Solid-Phase Grain Boundary Wetting in the Co-Cu System, *J. Mater. Sci.*, 2010, **45**, p 4271–4275
22. B.B. Straumal, A.S. Gornakova, Y.O. Kucheev, B. Baretzky, and A.N. Nekrasov, Grain Boundary Wetting by a Second Solid Phase in the Zr-Nb Alloys, *J. Mater. Eng. Perform.*, 2012, **21**, p 721–724
23. B.B. Straumal, S.G. Protasova, A.A. Mazilkin, G. Schütz, E. Goering, B. Baretzky, and P.B. Straumal, Ferromagnetism of Zinc Oxide Nanograined Films, *JETP Lett.*, 2013, **97**, p 367–377
24. B.B. Straumal, Y.O. Kucheev, L.I. Efron, A.L. Petelin, J. Dutta Majumdar, and I. Manna, Complete and Incomplete Wetting of Ferrite Grain Boundaries by Austenite in the Low-Alloyed Ferritic Steel, *J. Mater. Eng. Perform.*, 2012, **21**, p 667–670
25. A.A. Mazilkin, G.E. Abrosimova, S.G. Protasova, B.B. Straumal, G. Schütz, S.V. Dobatkin, and A.S. Bakai, Transmission Electron Microscopy Investigation of Boundaries Between Amorphous "Grains" in $Ni_{50}Nb_{20}Y_{30}$ Alloy, *J. Mater. Sci.*, 2011, **46**, p 4336–4342
26. T.B. Massalski, Ed., *Binary Alloy Phase Diagrams*, 2nd ed., ASM International, Materials Park, 1990
27. A.B. Straumal, B.S. Bokstein, A.L. Petelin, B.B. Straumal, B. Baretzky, A.O. Rodin, and A.N. Nekrasov, Apparently Complete Grain Boundary Wetting in Cu-In Alloys, *J. Mater. Sci.*, 2012, **47**, p 8336–8343
28. V.N. Semenov, B.B. Straumal, V.G. Glebovsky, and W. Gust, Preparation of Fe-Si Single Crystals and Bicrystals for Diffusion Experiments by the Electron-Beam Floating Zone Technique, *J. Crystal Growth*, 1995, **151**, p 180–186
29. E.I. Rabkin, V.N. Semenov, L.S. Shvindlerman, and B.B. Straumal, Penetration of Tin and Zinc along Tilt Grain Boundaries 43[100] in Fe-5 at.%Si Alloy: Premelting Phase Transition?, *Acta. Metal. Mater.*, 1991, **39**, p 627–639
30. O.I. Noskovich, E.I. Rabkin, V.N. Semenov, B.B. Straumal, and L.S. Shvindlerman, Wetting and Premelting Phase Transitions in 38 [100] Tilt Grain Boundaries in (Fe-12 at.% Si) Zn Alloy in the Vicinity of the A2-B2 Bulk Ordering in Fe-12 at.%Si Alloy, *Acta. metal. Mater.*, 1991, **39**, p 3091–3098
31. B.B. Straumal, L.M. Klinger, and L.S. Shvindlerman, The Effect of Crystallographic Parameters of Interphase Boundaries on Their Surface Tension and Parameters of the Boundary Diffusion, *Acta Metal.*, 1984, **32**, p 1355–1364
32. G. Hasson, J.-Y. Boos, and I. Herbeuval, Theoretical and Experimental Determinations of Grain Boundary Structure and Energies: Correlation with Various Experimental Results, *Surf. Sci.*, 1972, **31**, p 115–121
33. G. Hasson and C. Goux, Interfacial Energies of Tilt Boundaries in Aluminium. Experimental and Theoretical Determination, *Scr. Met.*, 1971, **5**, p 889–894
34. A. Otsuki, Variation of Energies of Aluminium [001] Boundaries with Misorientation and Inclination, *Mater. Sci. Forum*, 1996, **207**, p 413–416
35. G. Dhalenne, M. Dechamps, and A. Revcolevschi, Relative Energies of (011) Tilt Boundaries in NiO, *J. Am. Ceram.*, 1982, **65**, p C11–C12
36. G. Dhalenne, A. Peccolevschi, and A. Gervais, Grain Boundaries in NiO. I. Relative Energies of ⟨001⟩ Tilt Boundaries, *Phys. Stat. Sol. A*, 1979, **56**, p 267–276
37. B.B. Straumal, S.A. Polyakov, and E.J. Mittemeijer, Temperature Influence on the Faceting of Sigma 3 and Sigma 9 Grain Boundaries in Cu, *Acta Mater.*, 2006, **54**, p 167–172
38. B.B. Straumal, A.S. Gornakova, V.G. Sursaeva, and V.P. Yashnikov, Second-Order Faceting-Roughening of the Tilt Grain Boundary in Zinc, *Int. J. Mater. Res.*, 2009, **100**, p 525–529
39. B.B. Straumal, B. Baretzky, O.A. Kogtenkova, A.S. Gornakova, and V.G. Sursaeva, Faceting-Roughening of Twin Grain Boundaries, *J. Mater. Sci.*, 2012, **7**, p 1641–1646